Superhump and outburst activity of the cataclysmic variable RZ LMi in the “*U*”- and optical passbands.

S. Shugarov, N. Katysheva, V. Krushevska, D.Chochol

Slovak Academy of Sciences, Tatranska Lomnica, Slovakia
Sternberg Astronomical Institute, Moscow University, Russia
Main Astronomical Observatory, Kyiv, Ukraine.

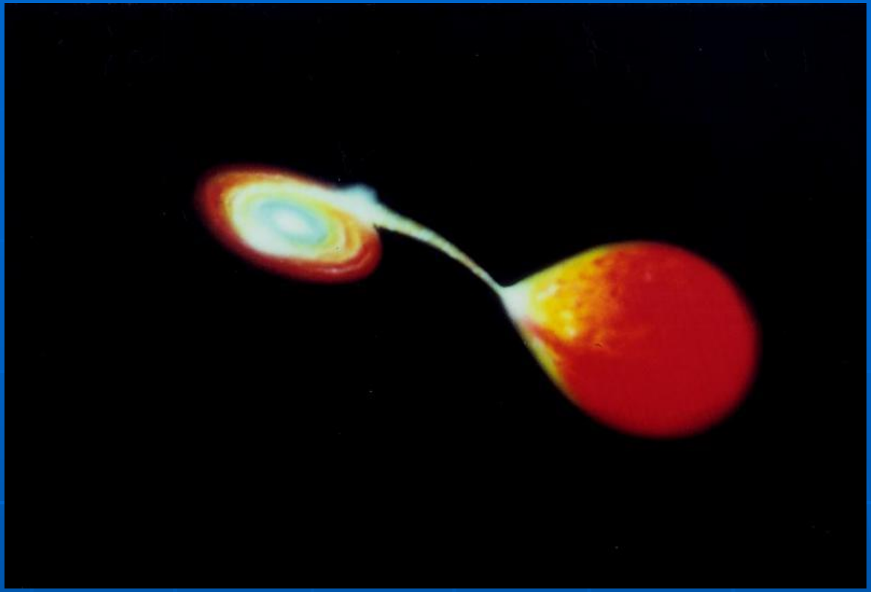

Cataclysmic variables (CVs) are close binaries, transferring matter from a red dwarf secondary onto a white dwarf (WD) primary. In the absence of a strong magnetic field overflowing matter forms an accretion disk around the WD. Distances between the components of CVs are about 1–2 solar radii. Their orbital periods are in the range from 1.5 h to several hours.

CV outbursts with the 1.5–8 mag amplitude, caused by a sudden brightening of the disk, last from a few days to a months. Then the disk returns to its normal state.

Spectroscopic observations during quiescence and outbursts of CVs are required to understand the physical processes taking place in such systems. Spectroscopic data are more difficult to obtain due to the weakness of CVs.

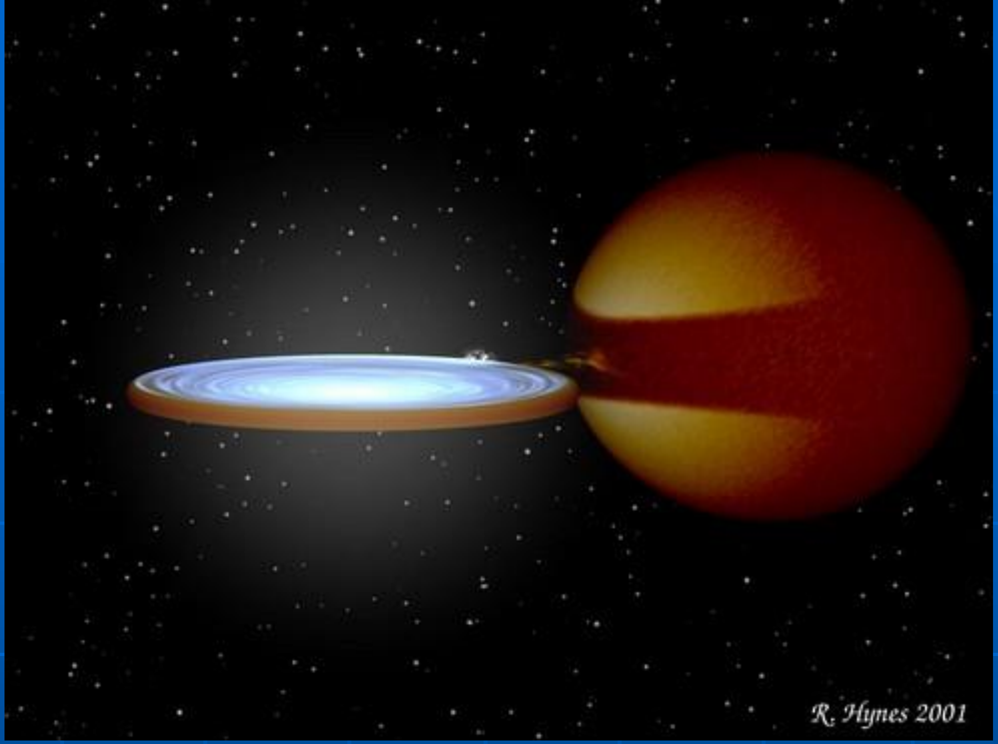

Nevertheless, a multicolor photometry allows us to understand the phenomena occurring in these close binaries. Earth-based observations in the *U*-passband, are very important because the accretion disk, the WD and other hot regions in the system significantly contribute to the radiation in this band.

The positions of dwarf novae (dNe) in the colour-colour diagram in quiescence (open circles) and outburst (filled circles). During outbursts the CVs in the diagram are shifted to the black body position due to the UV excess.

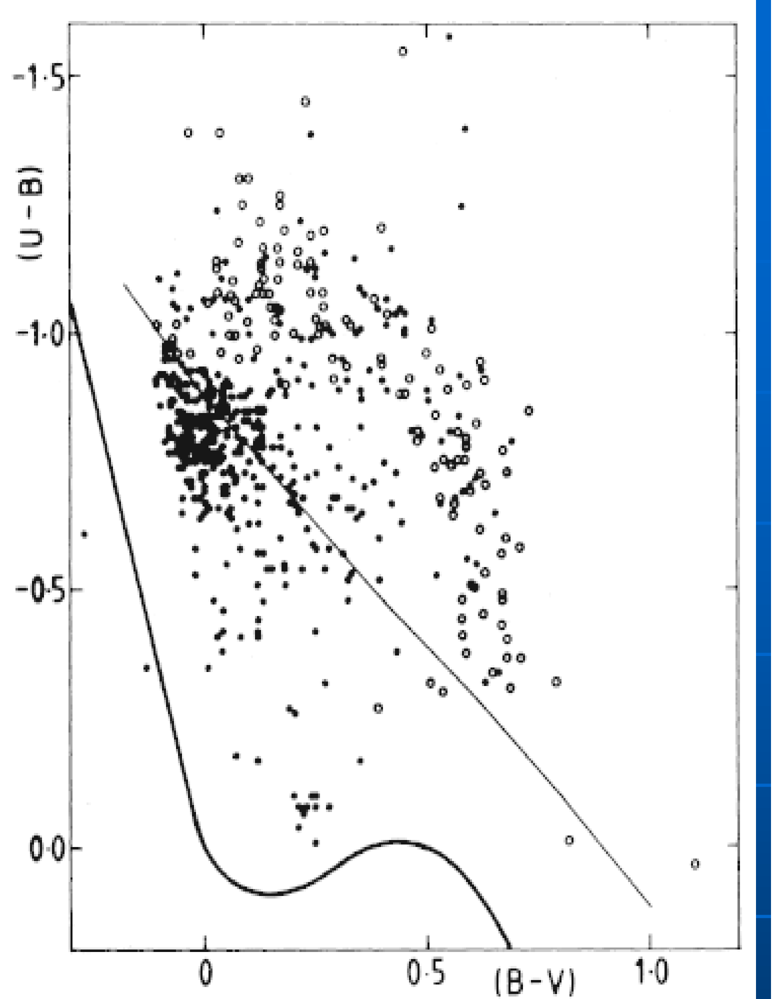

Fig. 1. Colour-colour diagram of dwarf novae. Open circles are observations at minimum. Filled circles are observations during outburst. The main-sequence and blackbody lines are shown.

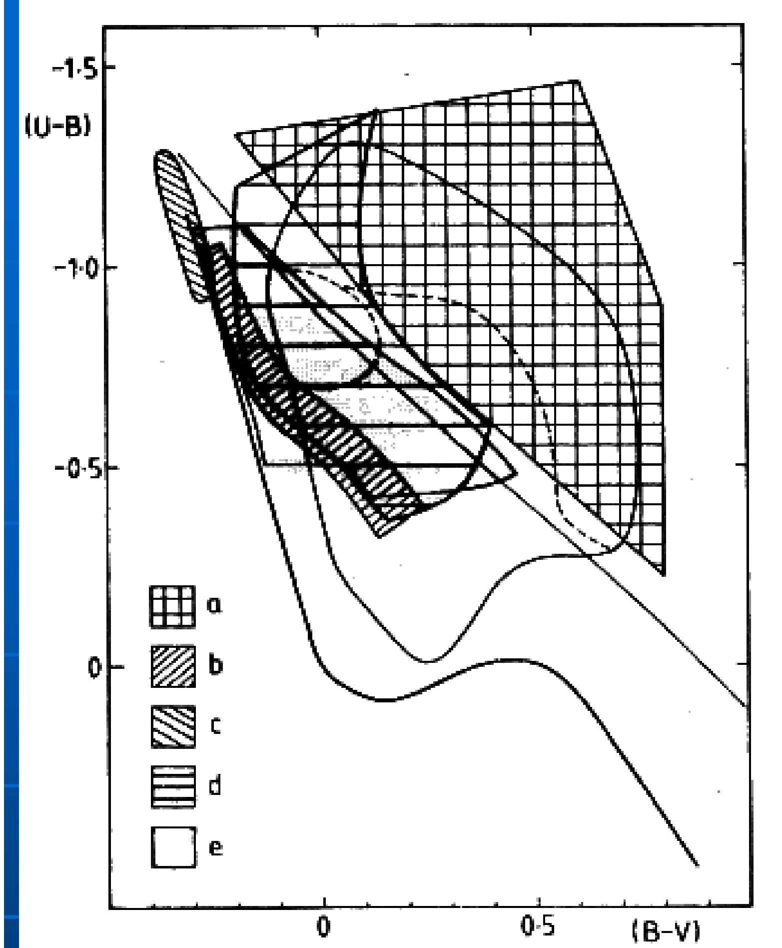

Fig. 4. Observational and theoretical (*U–B*, *B–V*) diagram. Models between the main-sequence and black body lines are optically thick. a) Tylenda 1981; b) Schwarzenberg-Czerny and Rozyczka 1977; c) Herter *et al.* 1979; d) Schwarzenberg-Czerny 1981; Mayo *et al.* 1980.

Figures from Echevarria & Jones (1983).

The theoretical (*U-B, B-V*) diagram.

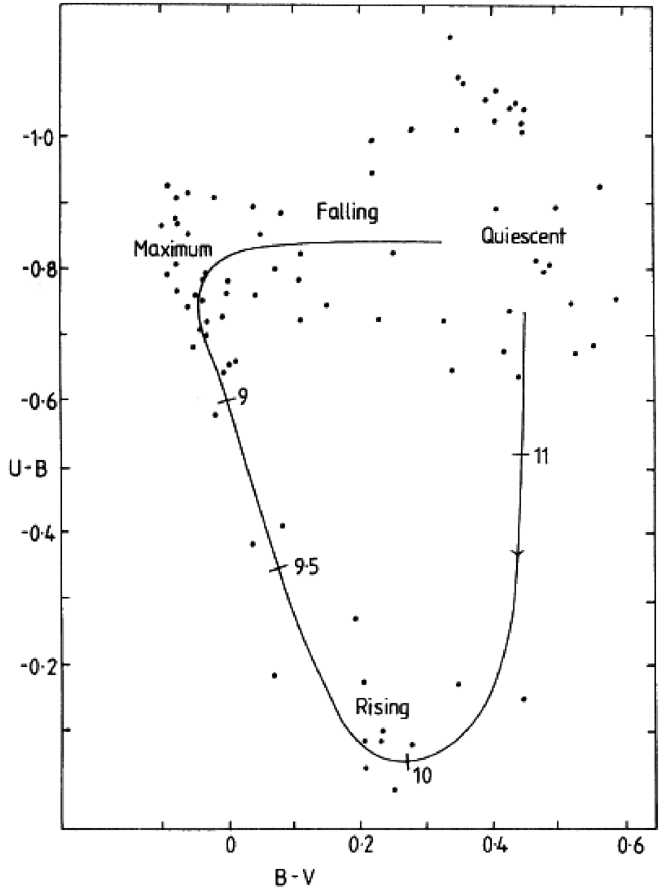

Figure 2. Path of SS Cyg in the two-colour plane. Each point represents a single observation. Observations have been taken from seven outbursts. The line is marked with the approximate *V* magnitude at the corresponding stage of the outburst.

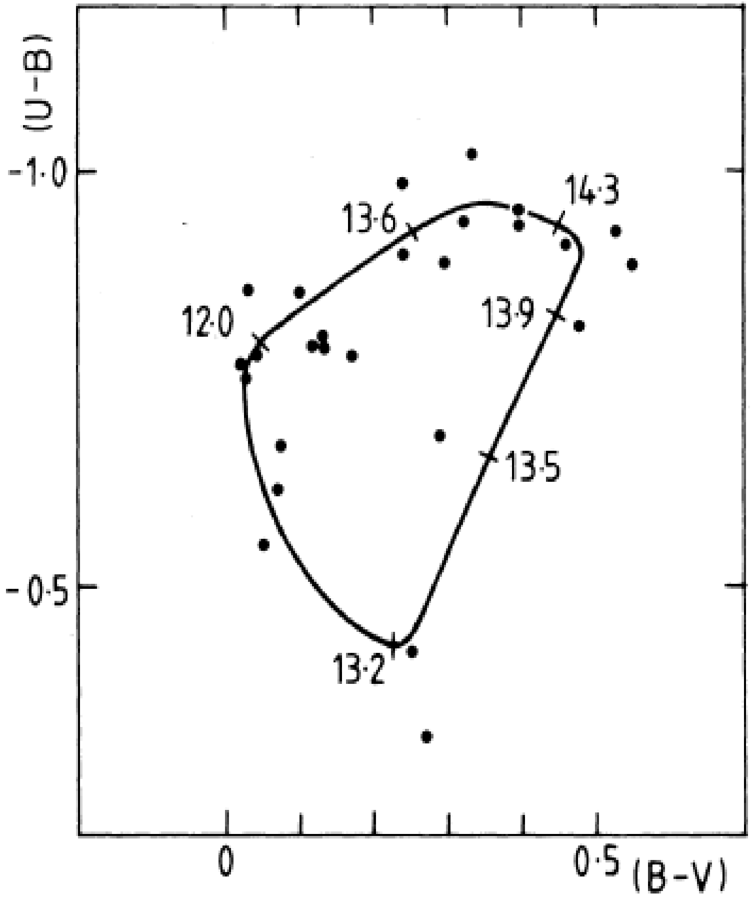

Fig. 2. Colour-colour diagram of AH Herculis. The *V* magnitude change during the outburst loop is shown.

The detailed investigations showed that the tracks of the stars in the (*U-B, B-V*) diagram are almost closed curves. The tracks of the famous dwarf nova SS Cyg (**left**) and other CVs AH Her (**right**).

Figures from Bailey (1980).

The tracks of the classical and X-ray novae in colour-luminosity and hardness-intensity diagrams at X-ray and EUV regions, are similar.

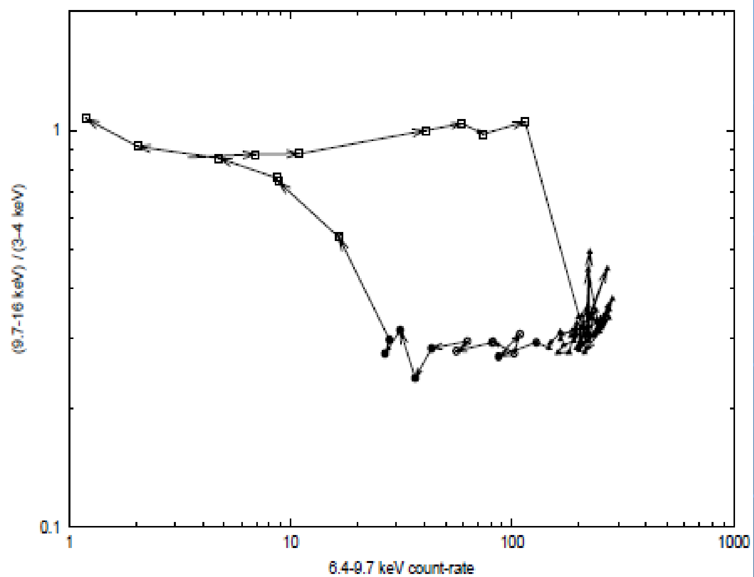

Evolution of Aql X-1 on X-ray color luminosity diagram. The

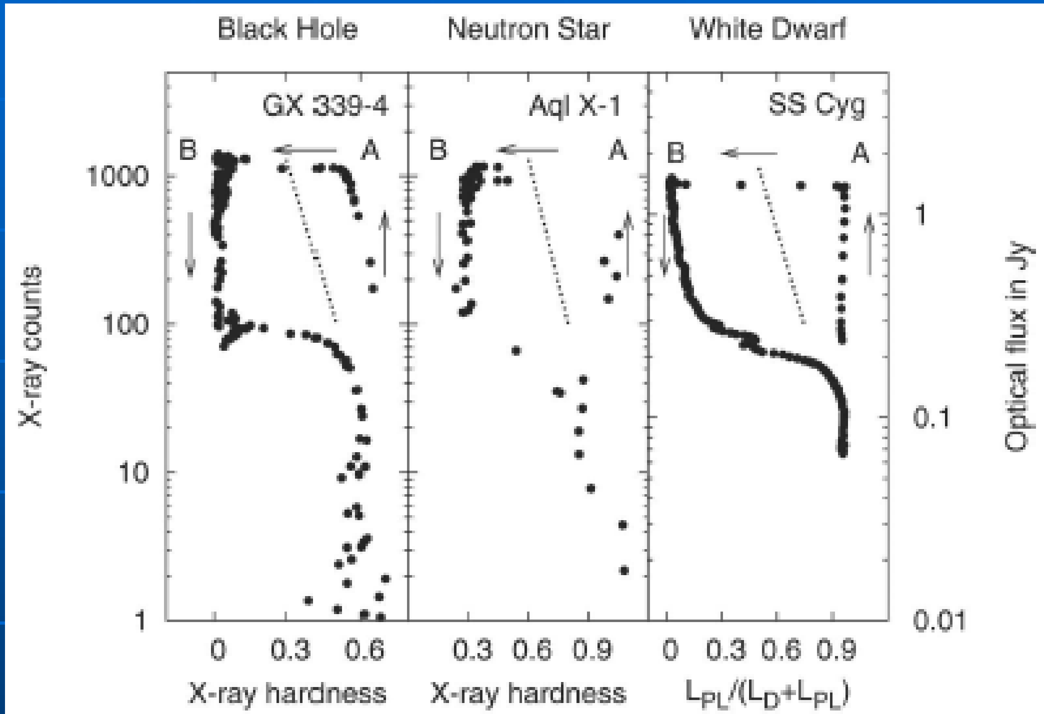

Fig. 1. Hardness-intensity diagrams for a black hole, a neutron star and a cataclysmic variables. Here, L_{PL} and L_D are is the X-ray and EUV luminosities respectively. Data is taken from Maitra & Bailyn (2004) and Wheatley et al. (2003). Figure reprinted from Körding et al. (2008) by permission of *Science*.

Figures from Maitra & Bailyn (2004) and Kording et al. (2008).

Tracks in the colour-magnitude diagrams of the classical novae DI Lac and Q Cyg. In DI Lac the small-amplitude outbursts occur in quiescence.

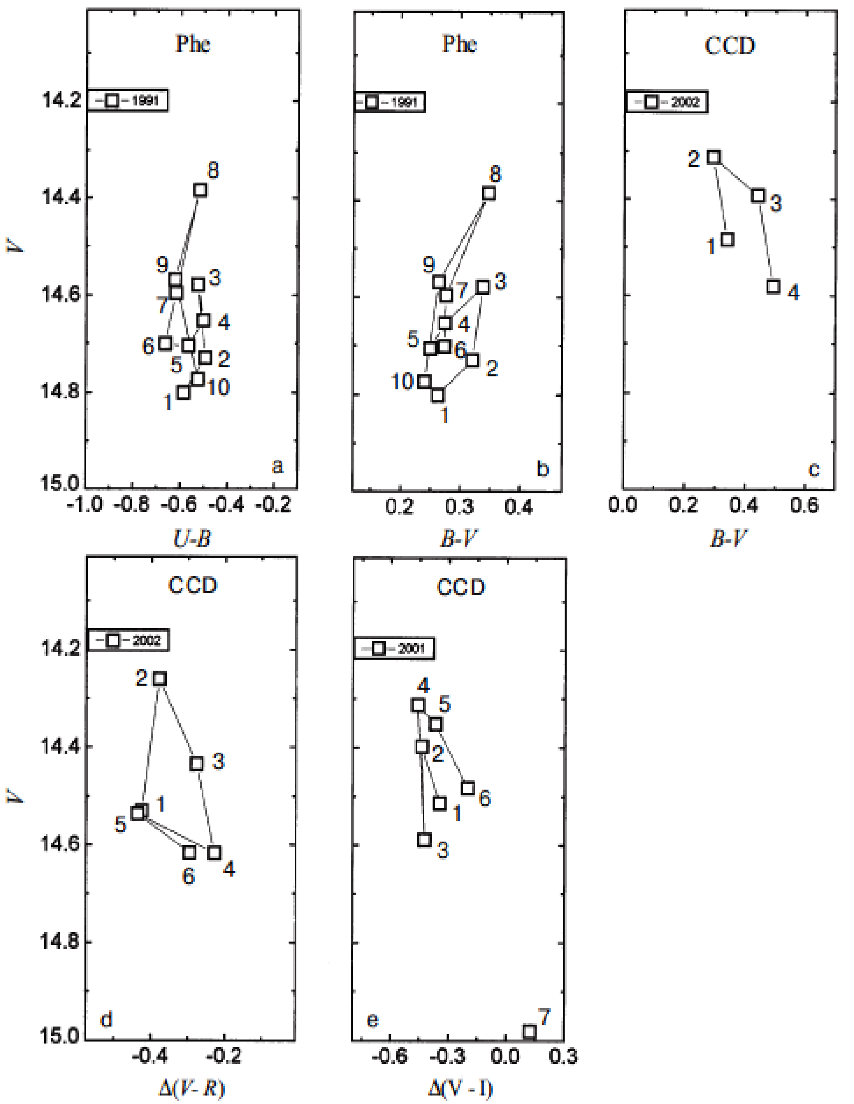

Fig. 8. Behavior of DI Lac flares on "magnitude–color" diagrams. The development of the flares is numbered in chronological order, "1" usually being close to the start of the ascending branch of the flare.

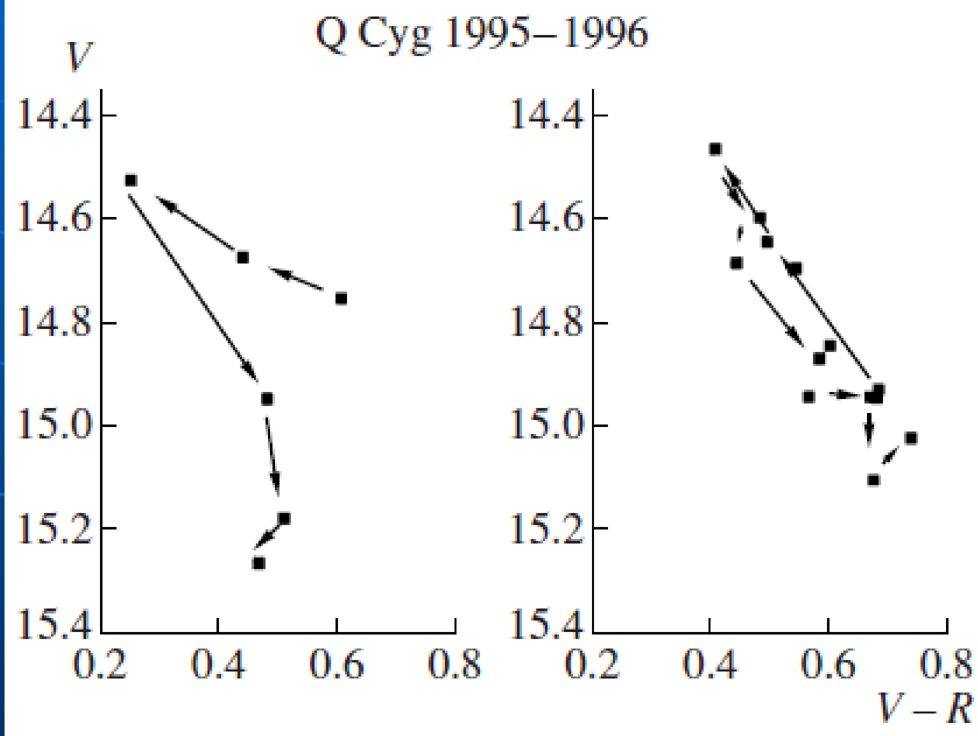

Fig. 14. Magnitude (*V*)–color (*V* – *R*) diagram for the two best observed outbursts of Q Cyg in 1995–1996.

Figures from Pavlenko et al. (2002, 2008).

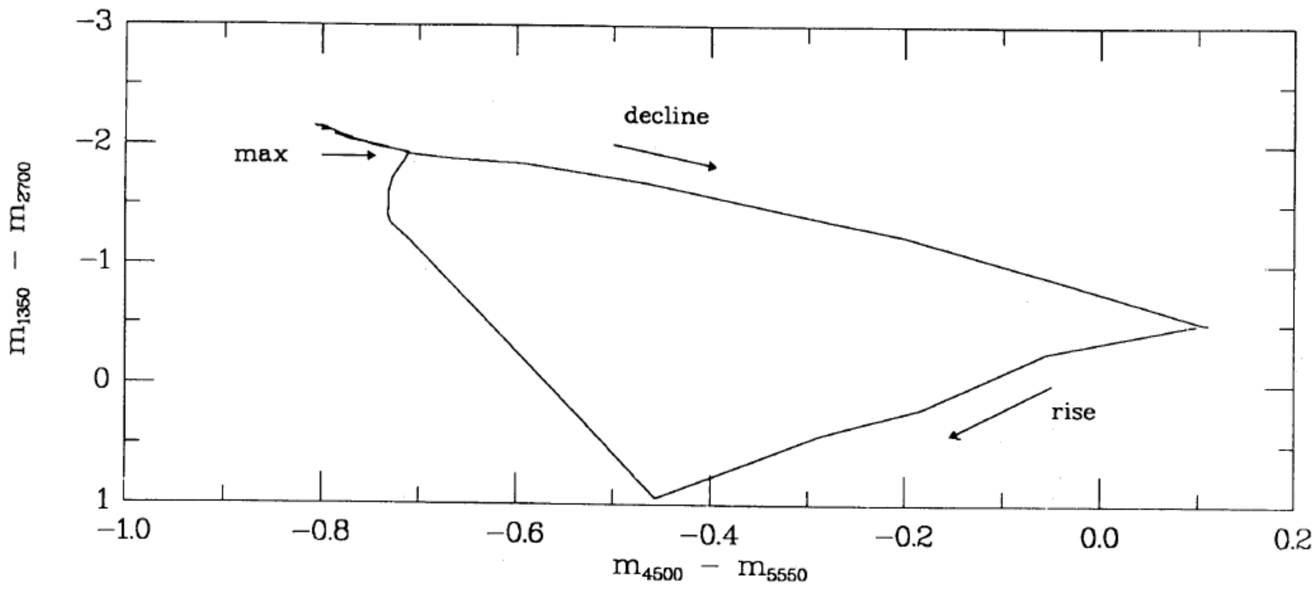

8.—Light and color curves for an outside-in eruption in a large disk (Model 4), with panels arranged as in Fi

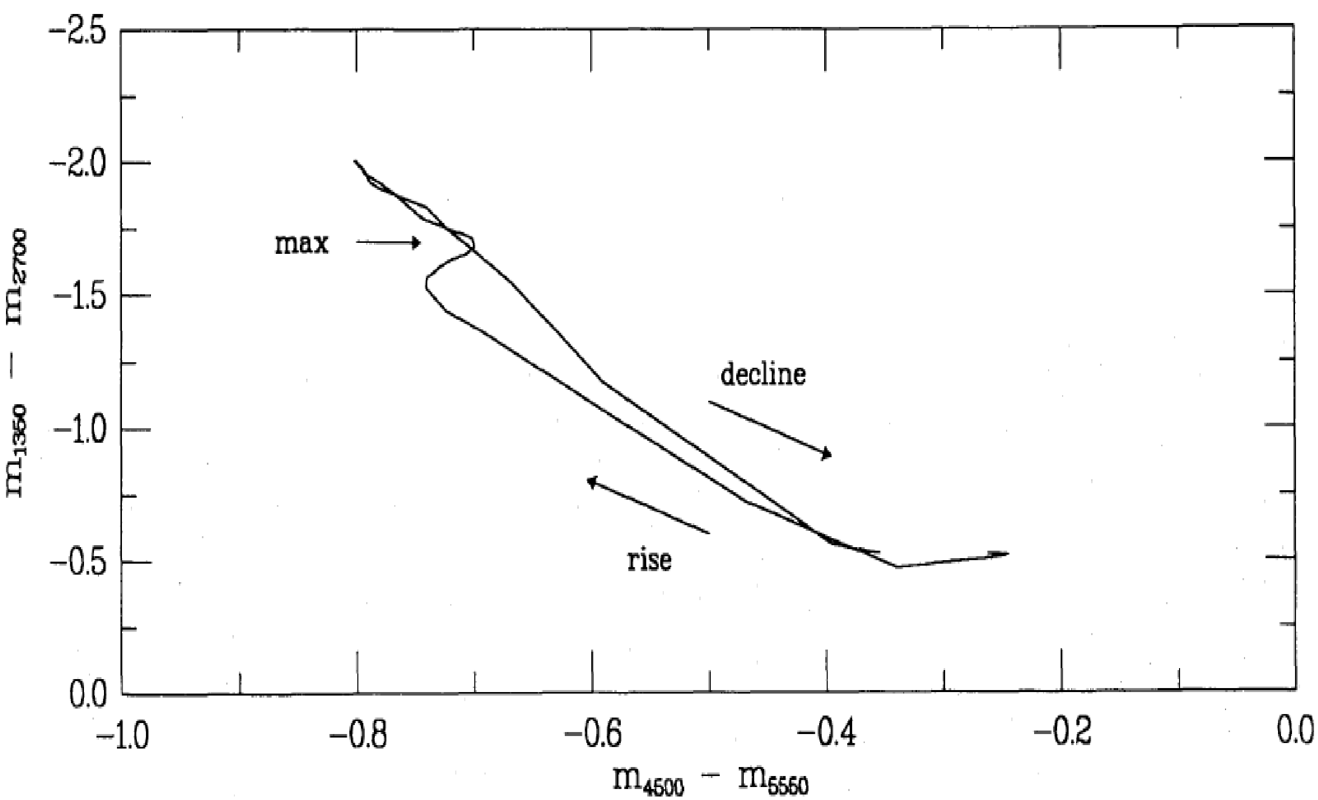

Theoretical model loops of CVs with different physical parameters (Cannizzo et al., 1987).

As seen in our slide 23, there is a good agreement with observations for CVs RZ LMi.

Fig. from Cannizzo & Kenyon (1987).

WZ Sge-type dwarf novae have recurrent time between superoutbursts tens of years. The colour-colour (*U-B, B-V)* and (*B-V, V-Rc)* diagrams of PNV J19150199+0719471 during its superoutburst in 2013. The number of days after maximum are indicated.

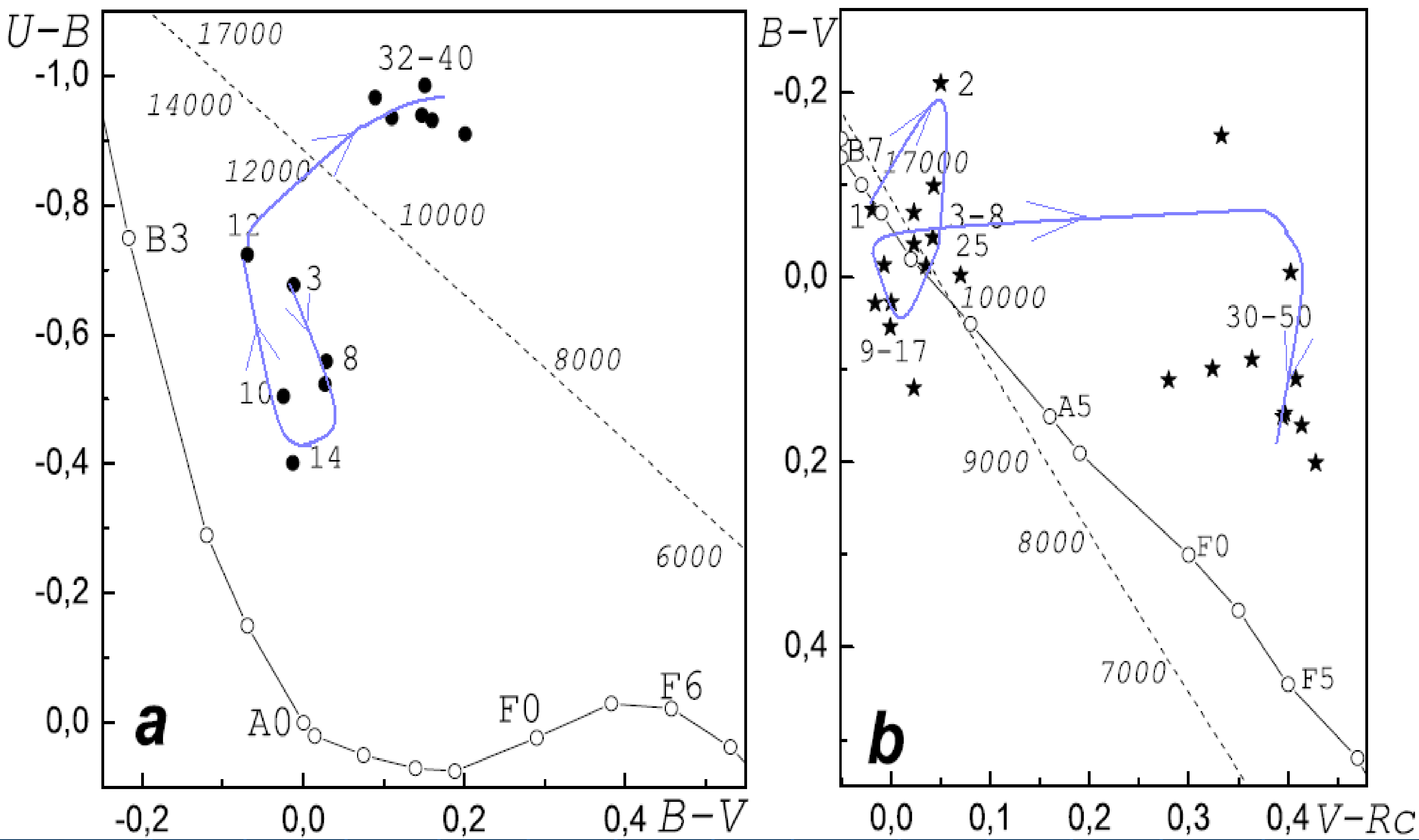

Figures from Golysheva & Shugarov (2014).

SU UMa-type dwarf novae (DNe) are a subclass of CVs. These stars show two types of outbursts: normal outbursts, with short recurrent time and superoutbursts with long (some months – one year) recurrent time.

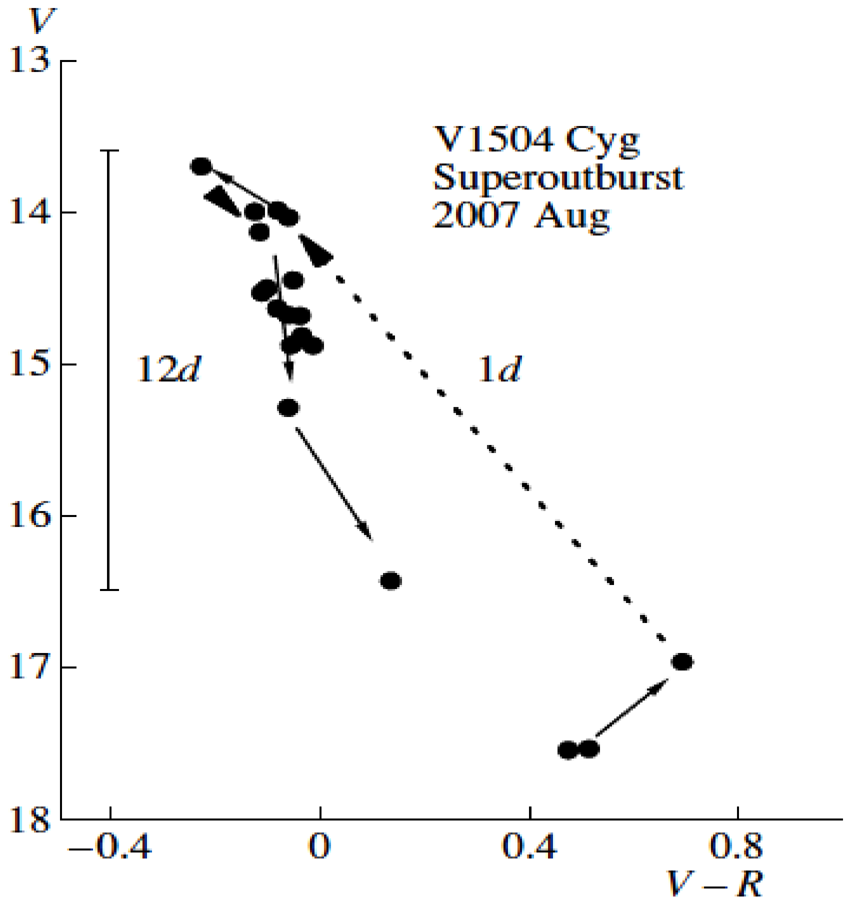

Fig. 4. Magnitude (*V*)–color (*V* – *R*) diagram for the V1504 Cyg superoutburst. The arrows show the chronology of outbursts.

During superoutbursts the superhumps with the period of a few percent longer than the orbital one are present.
The example of V1504 Cyg demonstrates the evolution in colour-magnitute diagram during superoutburst.

Fig. from Pavlenko et al. (2008).

ER UMa-stars are a subclass of SU UMa DNe with very short superoutburst interval lasting 1–2 months and amplitude of 3–4 mag.

RZ LMi is the ER UMa-type star with extremly short supercycle ~19 days. This object was discovered as a variable star with a strong *UV*-excess in Byurakan Observatory. It is one of the most enigmatic SU UMa-type DNa.

The light curve of the DNa RZ LMi. The object spends most of the time at a high state of brightness, the quiescence state is very short. The period of superhumps Psh=0.0593 d.

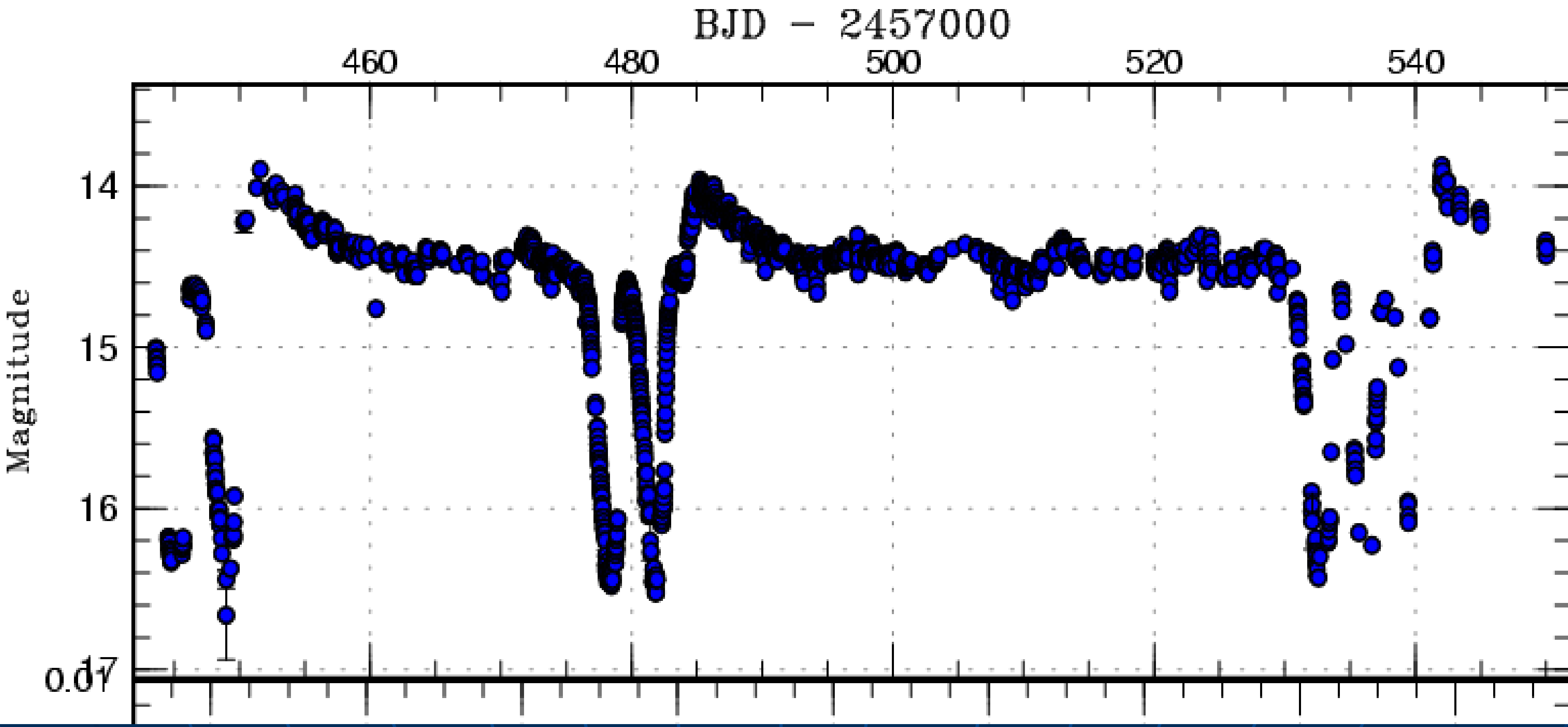

Figure from Kato et al. (2016).

We observed RZ LMi, using the 18–60 cm telescopes, from 2016, February till 2017, May in the *UBVRcIc*-bands (7000 *Rc*-frames, 4000 *U*-frames and about 2000 frames in each of the *BVIc*-passbands). The *Rc* light curve and colour indices during 15 months of observations:

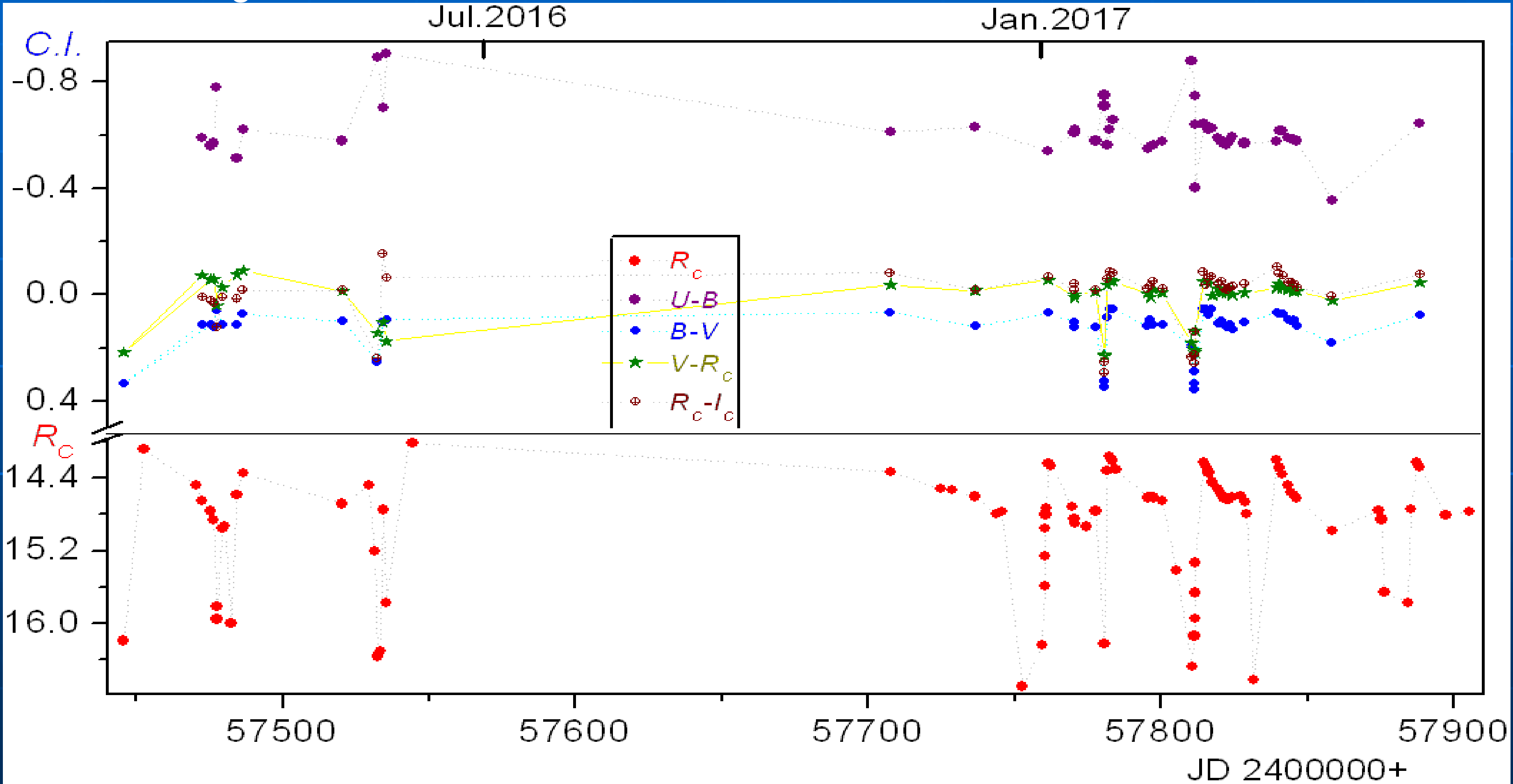

The *U-B* index is always negative. During the dips rapid changes of colour-indices are detected.

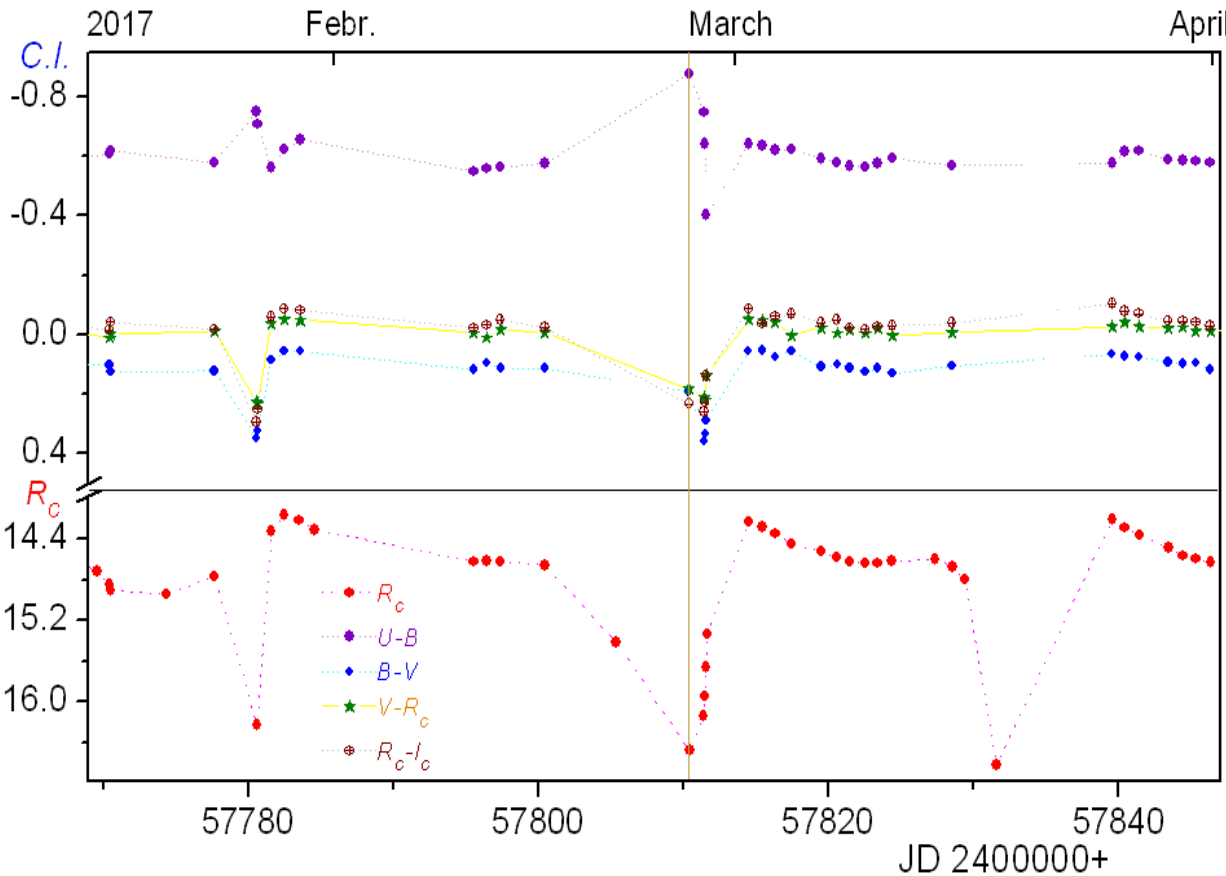

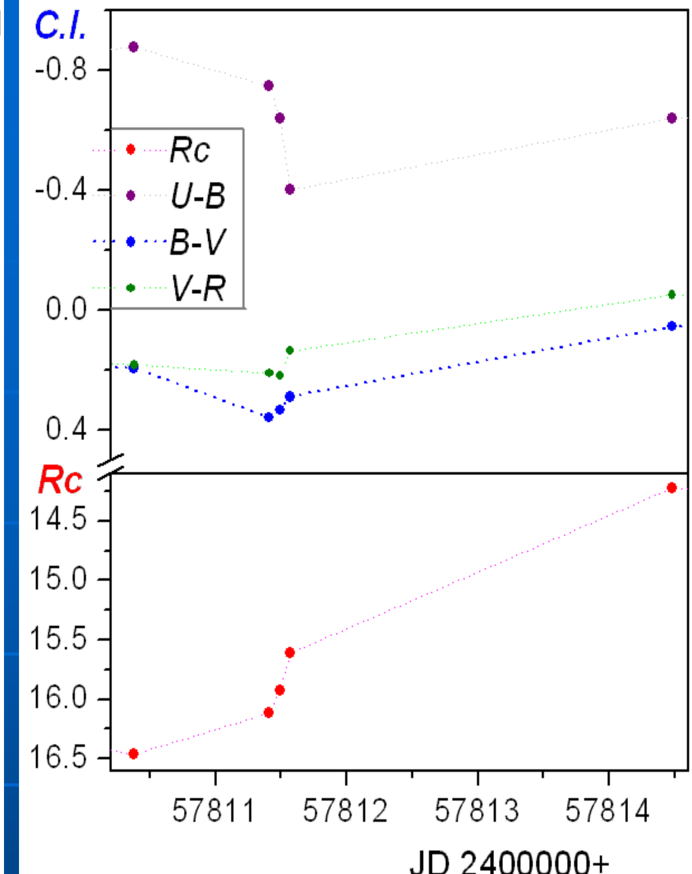

The *Rc* light curve and colour indices of RZ LMi in 2017. The object has the strongest *UV* excess at the minimum of brightness, then it drops sharply, and reaches a mean value at the maximum (**left**).

The detailed *Rc* light curve and colour indices of RZ LMi during 4 days after minimum. The *U-B* and *B-V* colour indices change in antiphase during the rise of brightness, at other times they show the same behaviour(**right**).

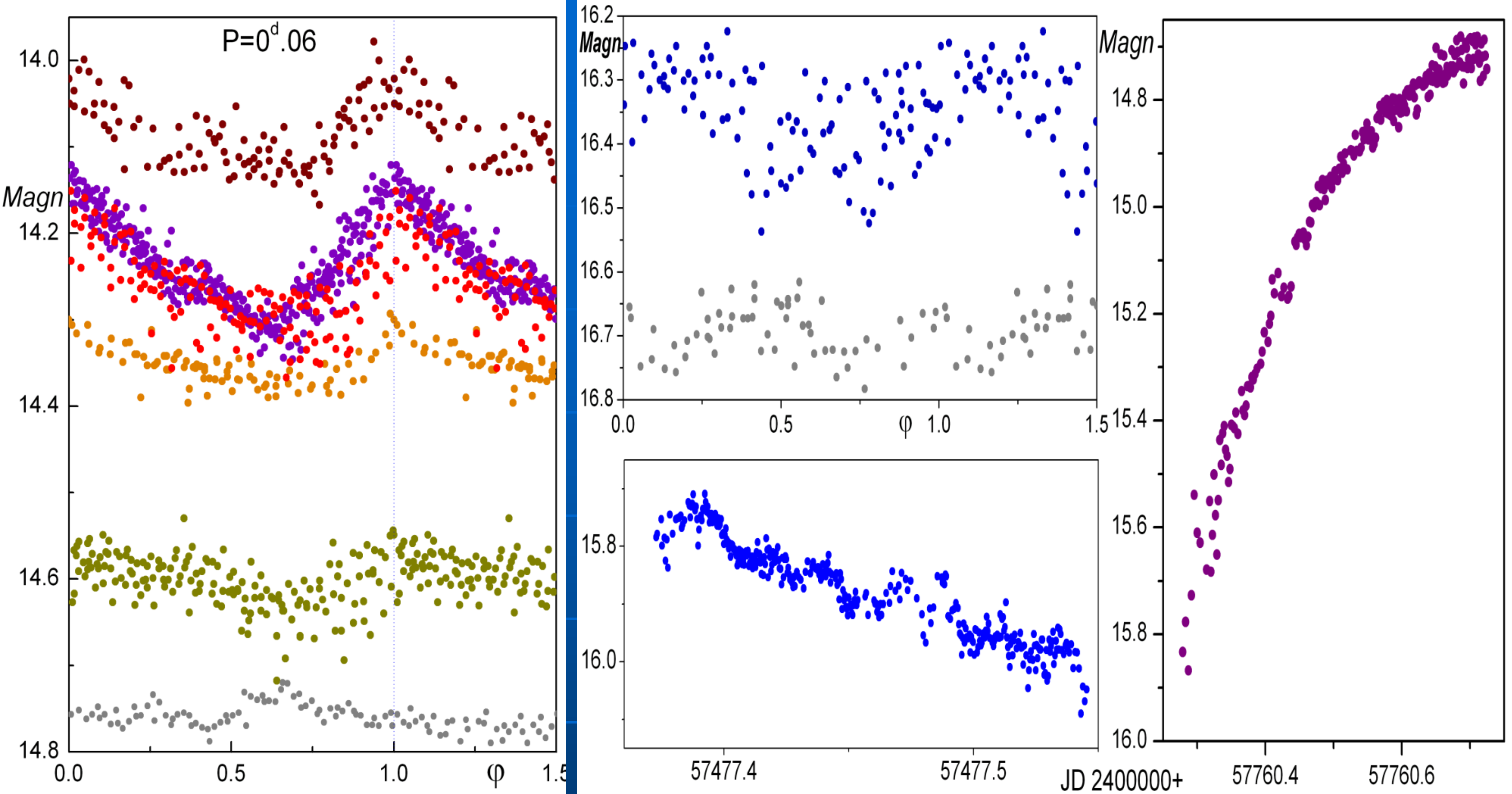

Left: The phase LCs at the beginning of superoutburst and the beginning of fading – there are 0.2-magnitude superhumps. Later the amplitude of superhumps diminishes to 0.1 mag and then its become less noticeable.

Right: In quiescence, on the rise and decline of brightness, the superhumps are either weak or absent. But non-periodic oscillations can be present.

Let's call the “Blue excess” the situation, when the shorter-wave radiation dominates, regardless of the passband. And the “Red excess” – the opposite case.

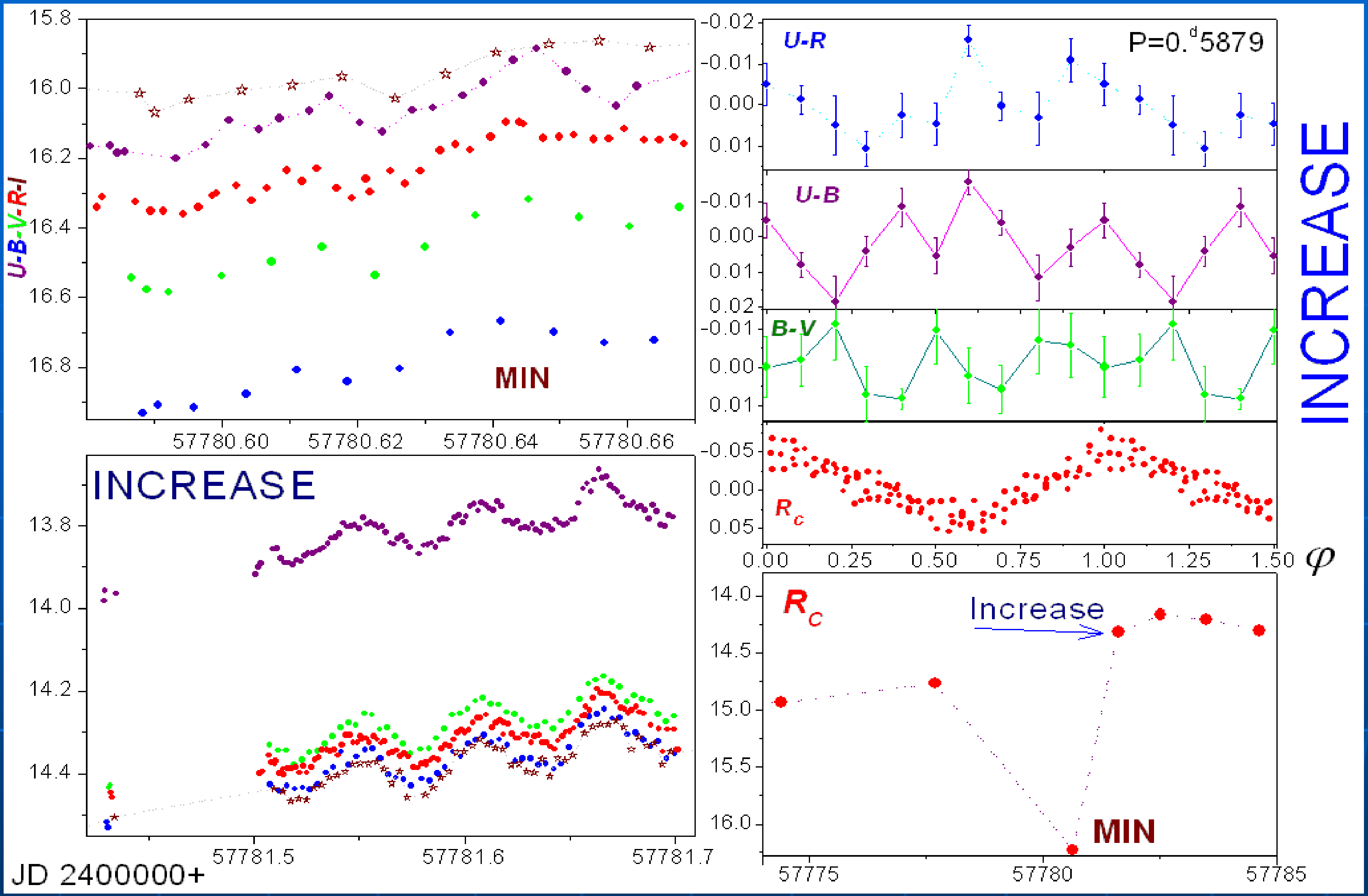

The nightly *UBVRcIc* LCs of RZ LMi at minimum and during the brightness increase.The quasi-periodic oscillations of brightness with approximate cycle 0.03 days are seen (**left**). The *Rc* and colour indices phase curves at JD 2457781, one day before maximum. The color-indices of superhumps do not explicitly correlate with their phase (**right**).

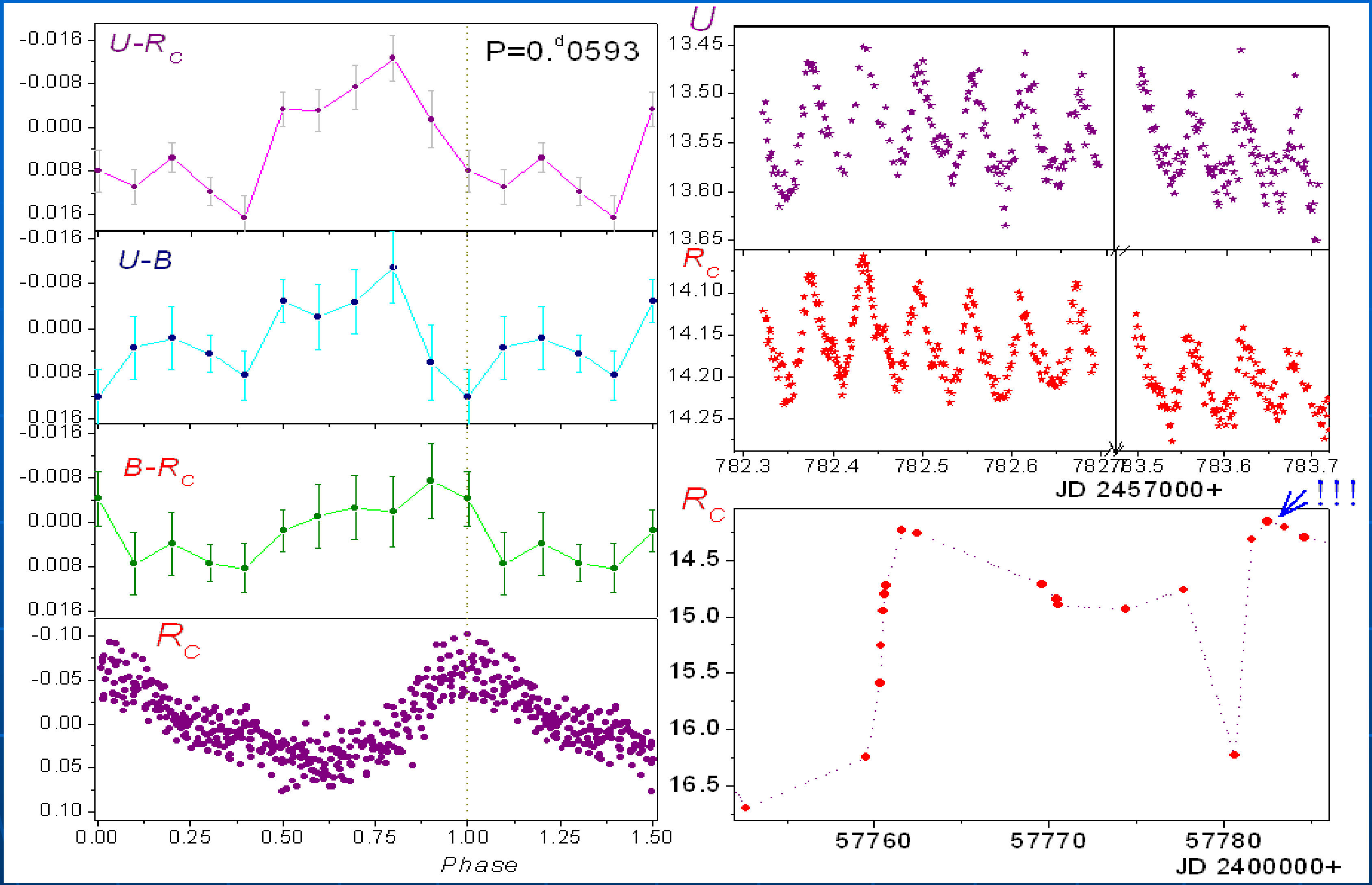

The phase and nightly light and colour curves at RZ LMi outburst maximum (JD 2457782). The superhumps amplitude reached 0.2 mag. The blue excess in *U-B* and *U-R*c phase curves reached maximum close to the minimum of the superhumps *R*c brightness. Colour index *B-R*c shows a slightly different behaviour.

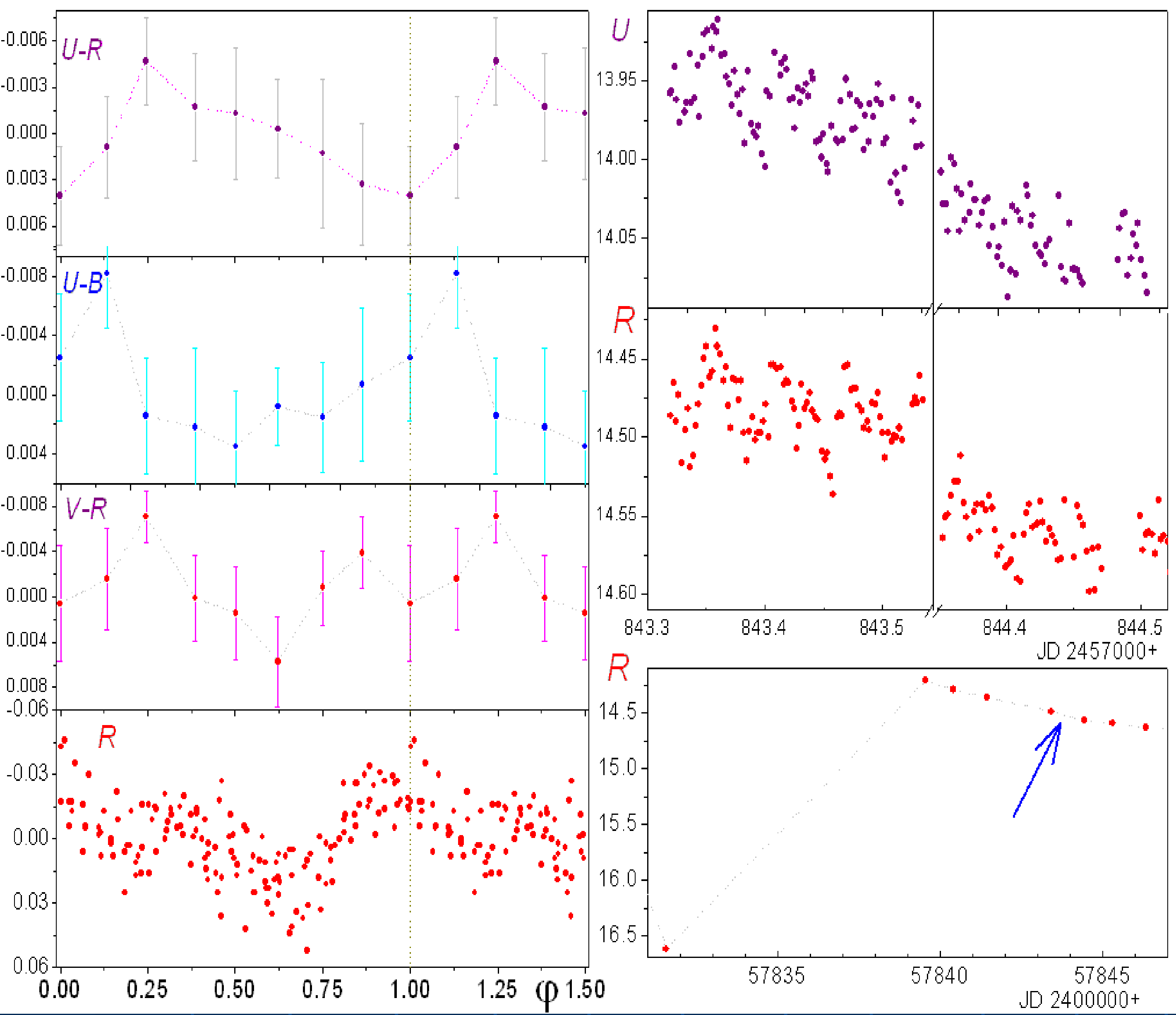

RZ LMi outburst fading. The super-hupms amplitude became three times less. The colour index *U-Rc* shows red excess at the superhumps maximum. But, since the amplitude of the colour-indices has decreased, it was difficult to make conclusions about their phase dependence.

The similar dependences of colour indices of superhumps were found by Neustroev et al. (2017) for SSS J122221.7-211525.

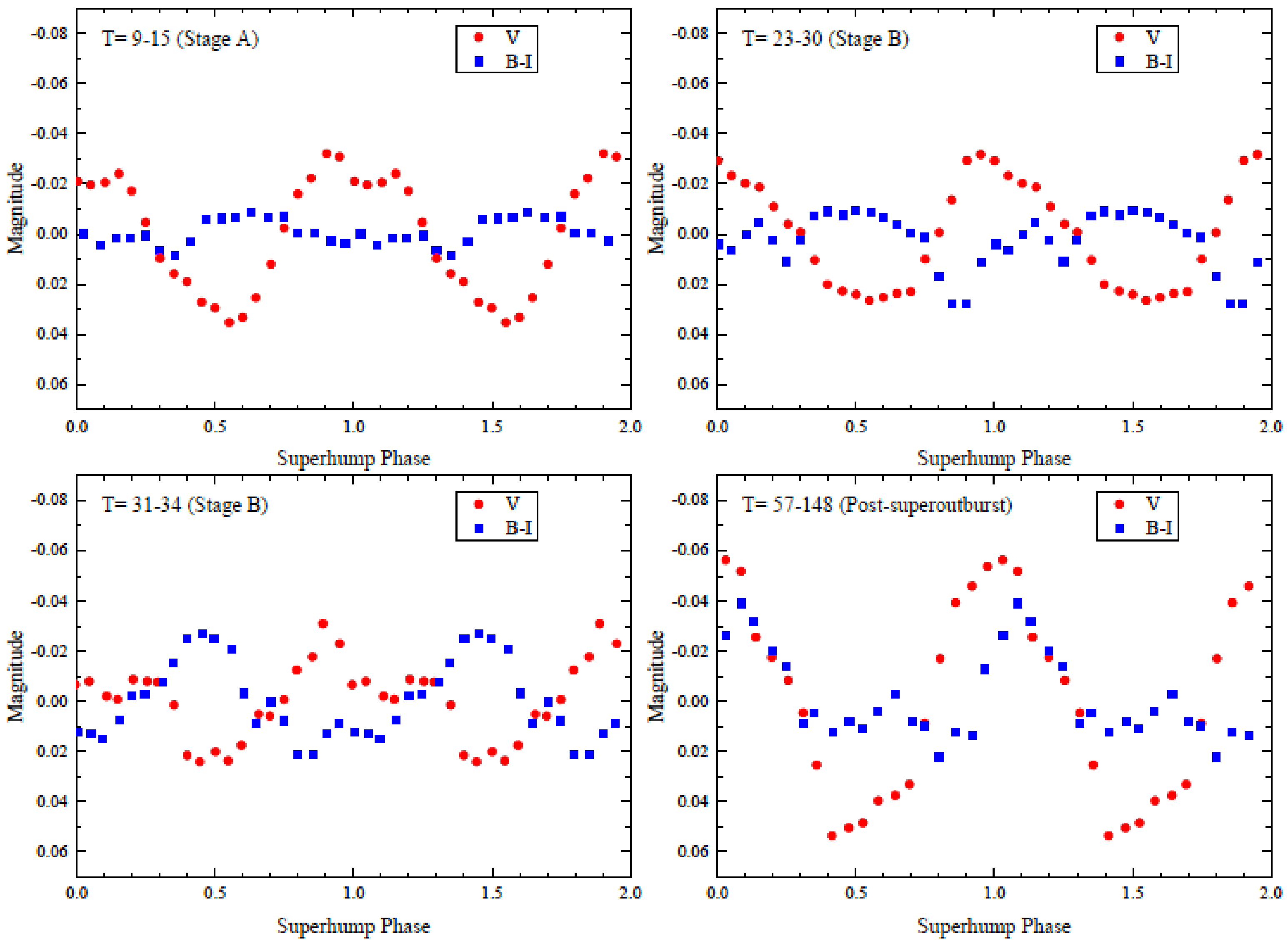

Figure 9. Phase-averaged *V* light curves and *B–I* colour variations of superhumps at different stages of the superoutburst of SSS J122222.

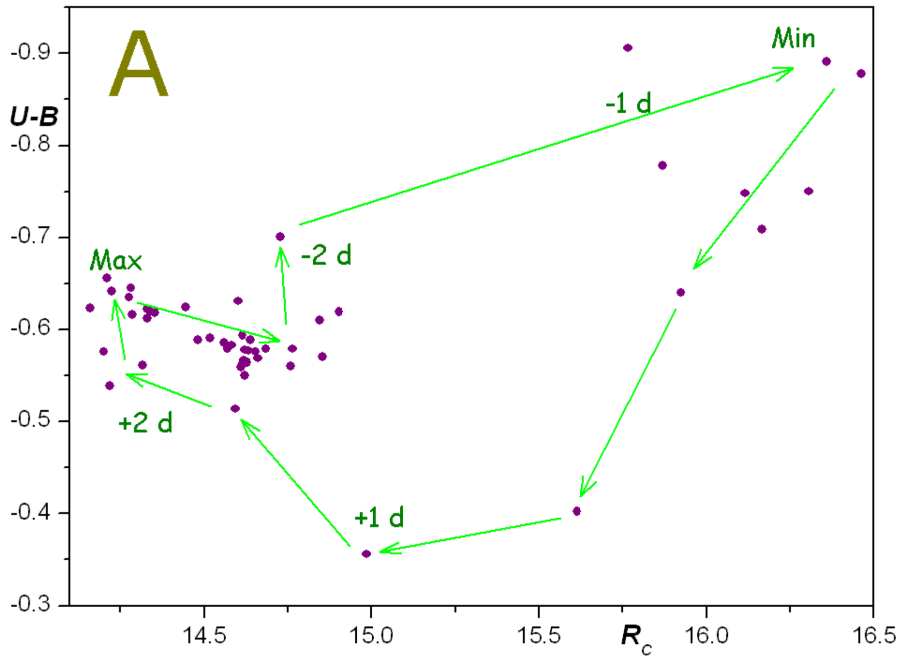

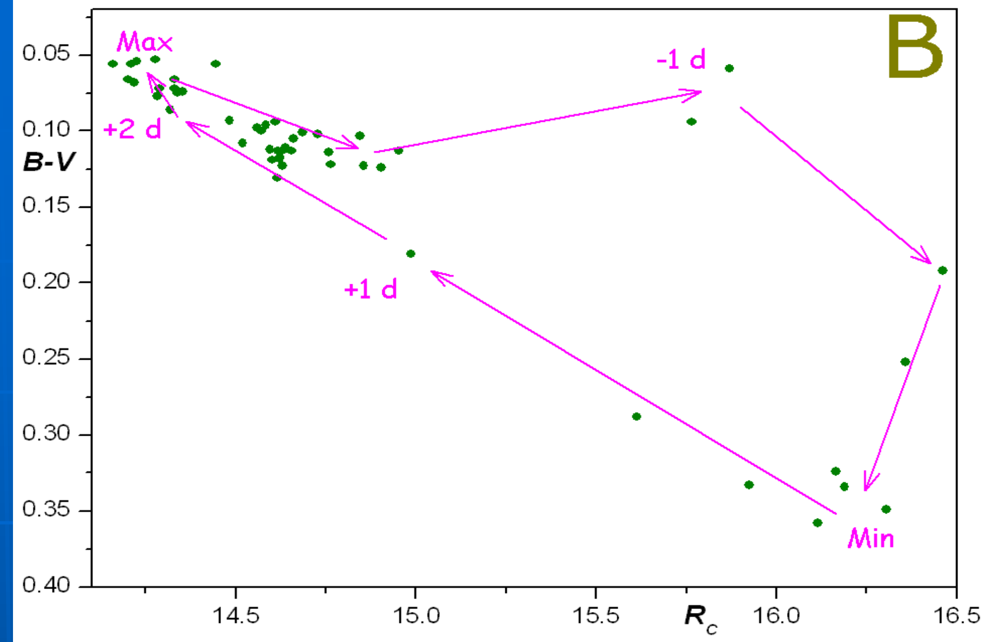

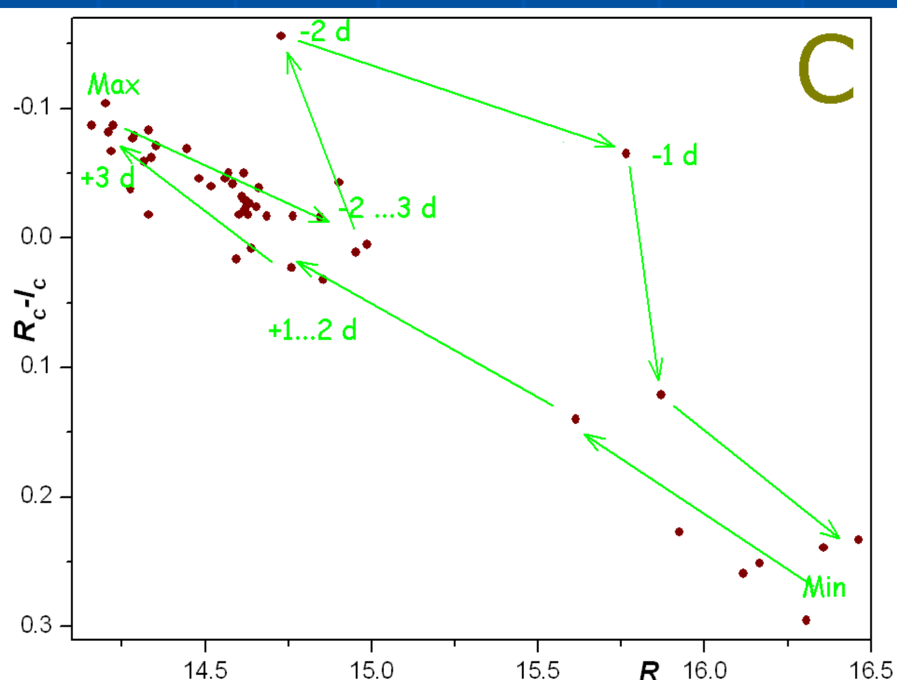

The tracks of RZ LMi in colour index versus *Rc* magnitude diagrams. The days are counted from the time of minimum.
A: The (*U-B*, *Rc*) diagram. The blue excess is observed at the minimum and during fading. **B:** The (*B-V*, *Rc*) diagram. The blue excess is observed during fading, red excess at minimum. **C:** The (*Rc-Ic* , *Rc*) diagram. Red excess is observed in quiescence.

The colour-colour diagrams are more informative.

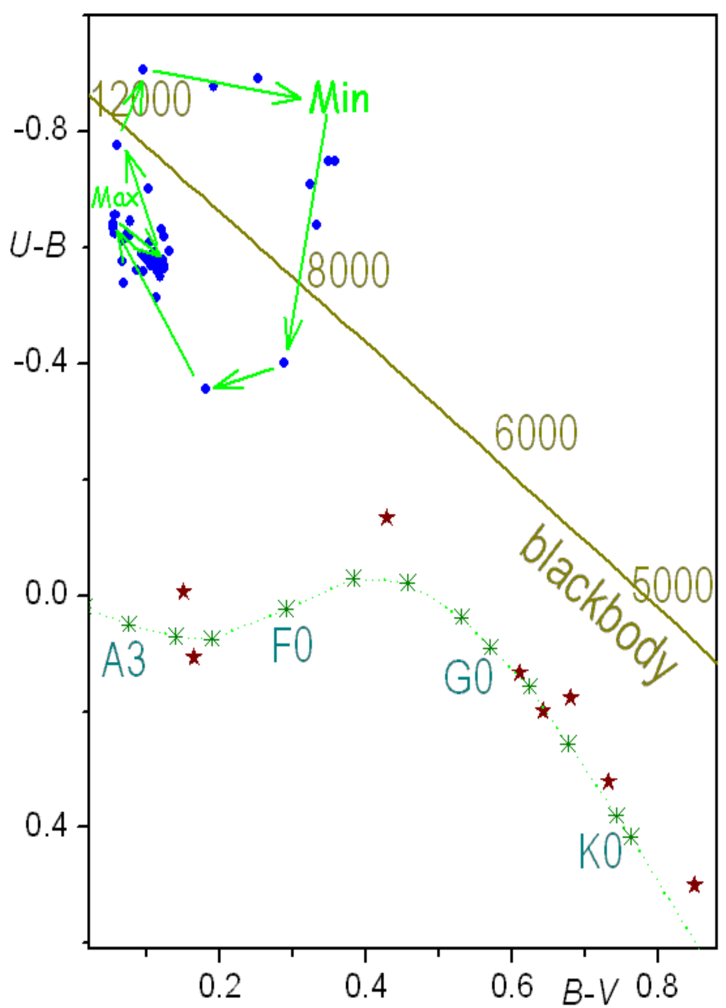

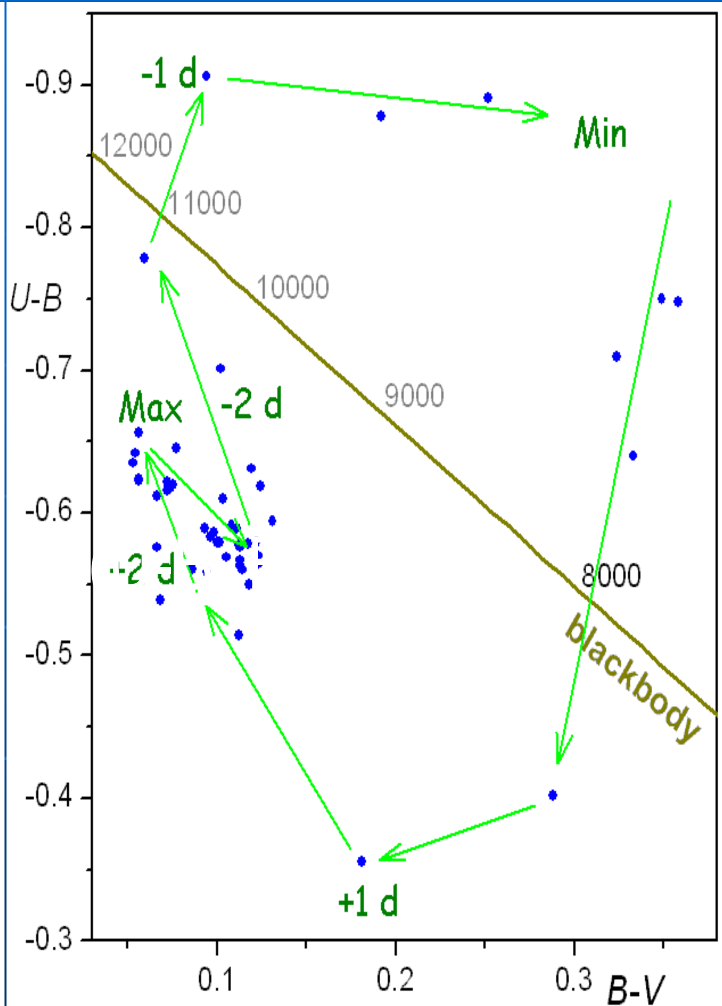

In the (*U-B*, *B-V*) diagrams the main and black body sequences are drawn. The asterisks show the position of neighbouring field stars.

The interstellar extinction is small, as expected for the galactic latitude of +51 degrees.

The track of RZ LMi in the (*U-B*, *B-V*) diagram. The blue excess in *U-B* reached maximum one day before the minimum and at the minimum of brightness.

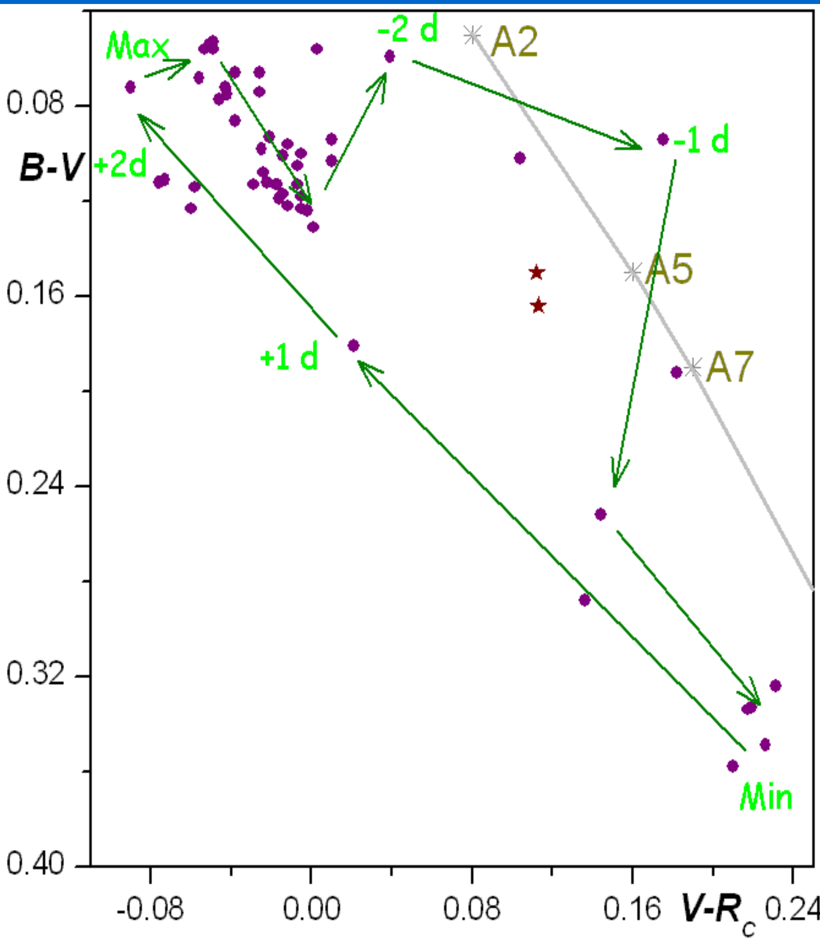

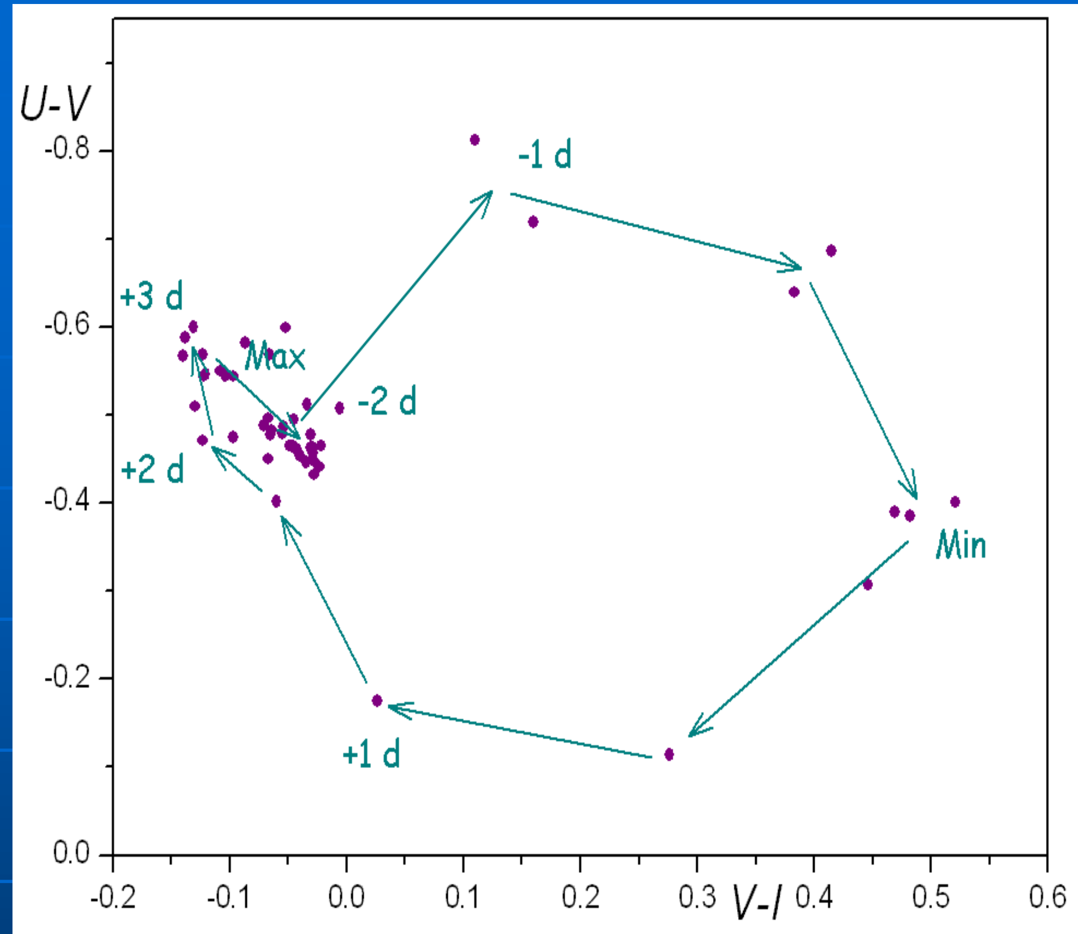

Left: The track of RZ LMi in the (*V-Rc, B-V)* diagram. The blue excess is observed at outburst maximum, the red excess in minimum.
Right: The track of RZ LMi in the *(U-V, V-Ic)* diagram. The track shows a very wide loop with a large blue excess during fading from maximum.

The reason for such changes of color indices can be the following. At minimum the accretion disk around the white dwarf has a small size. The inner regions of the disk re-emit the UV energy from the WD, which leads to a significant blue excess in an inactive phase. Around maximum the increased accretion disk size gives larger contribution to the total radiation of the system. The average temperature of the outer parts of the disk is lower than its inner parts.

So, the largest UV excess we can see in quiescence.

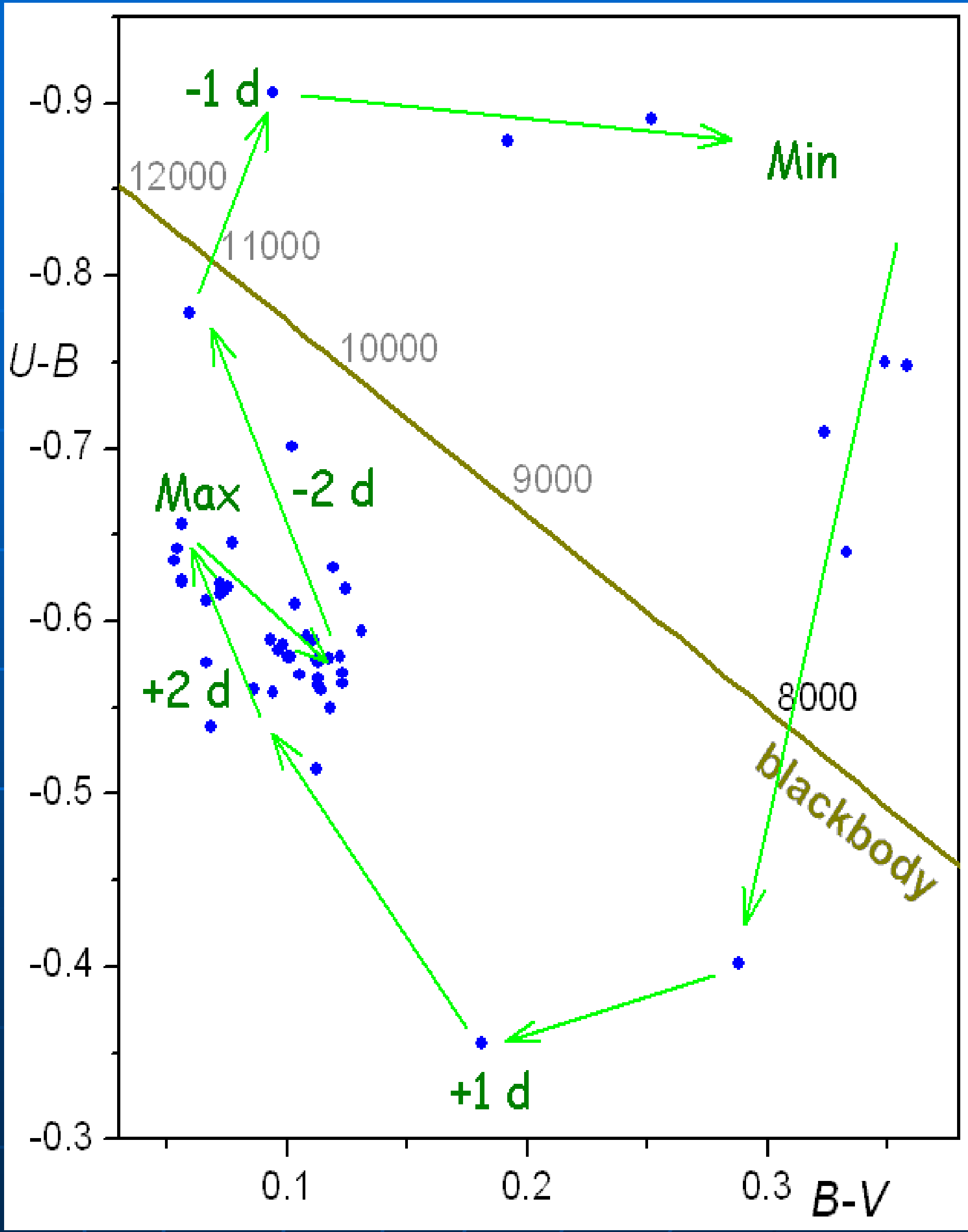

The position of RZ LMi on the (*Rc-Ic, Rc)* diagram depends on radiation of the cooler parts of the disk, with the maximum of its emission in the *Rc, Ic* passbands. The contribution of the WD and hot inner disk is smaller for infrared region and loops have another forms. The object has red excess at the minimum and blue excess at the maximum of brightness.

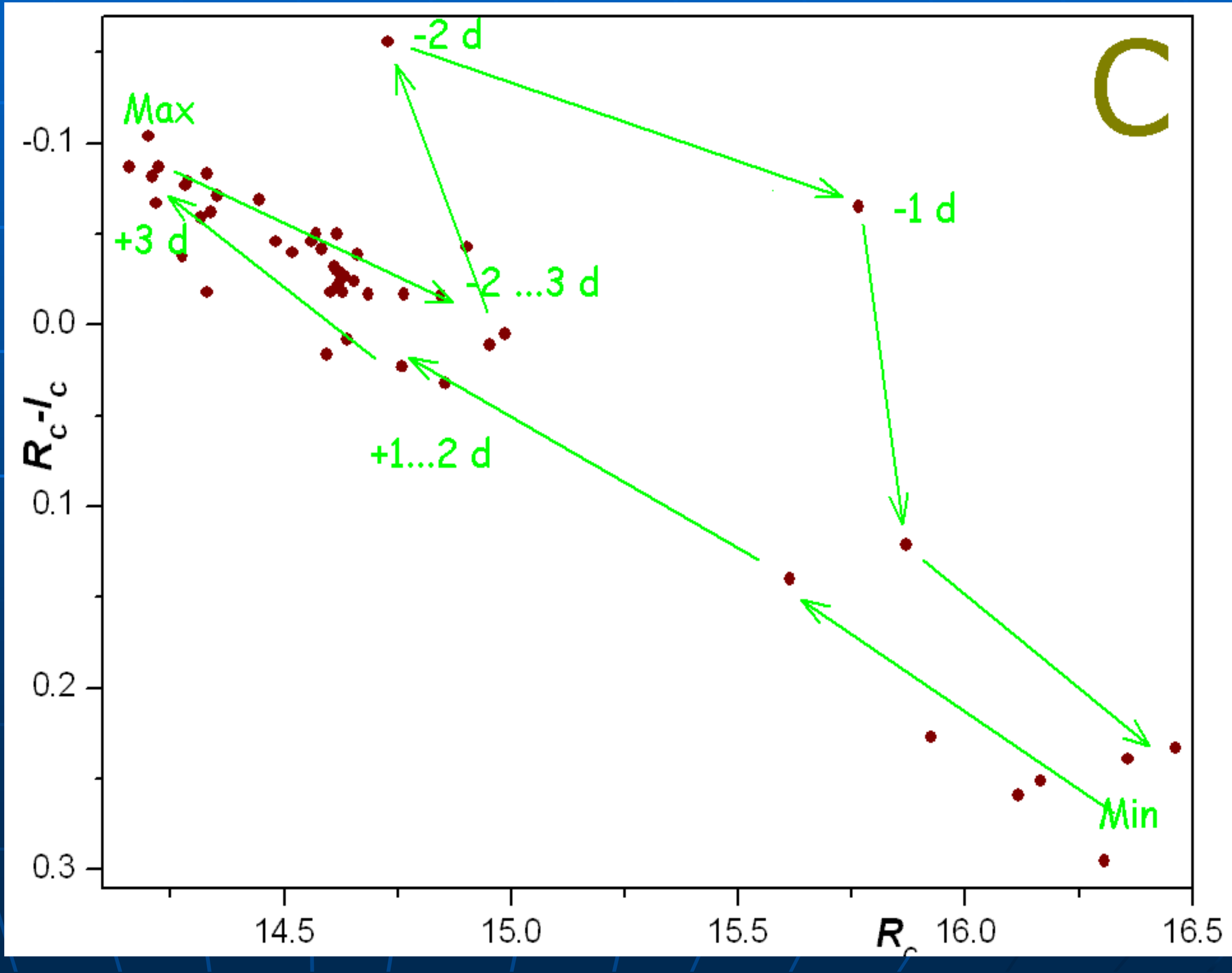

Cannizzo & Kenyon (1987) and Bailey (1980) came to similar conclusions.

Superhump colours are the bluest at a superhump minimum and the reddest at a superhump maximum. Many authors, e.g. Hassall (1985), Warner (1995), van Amerongen et al. (1987) considered the changes of superhump colour indices.

Warner:

"This is more pronounced towards shorter wavelengths: the flux distribution is almost flat in *B* and *V*. Thus there appears to be an inverse correlations between colour temperature and brightness, implying substantial changes in area of superhump light source."

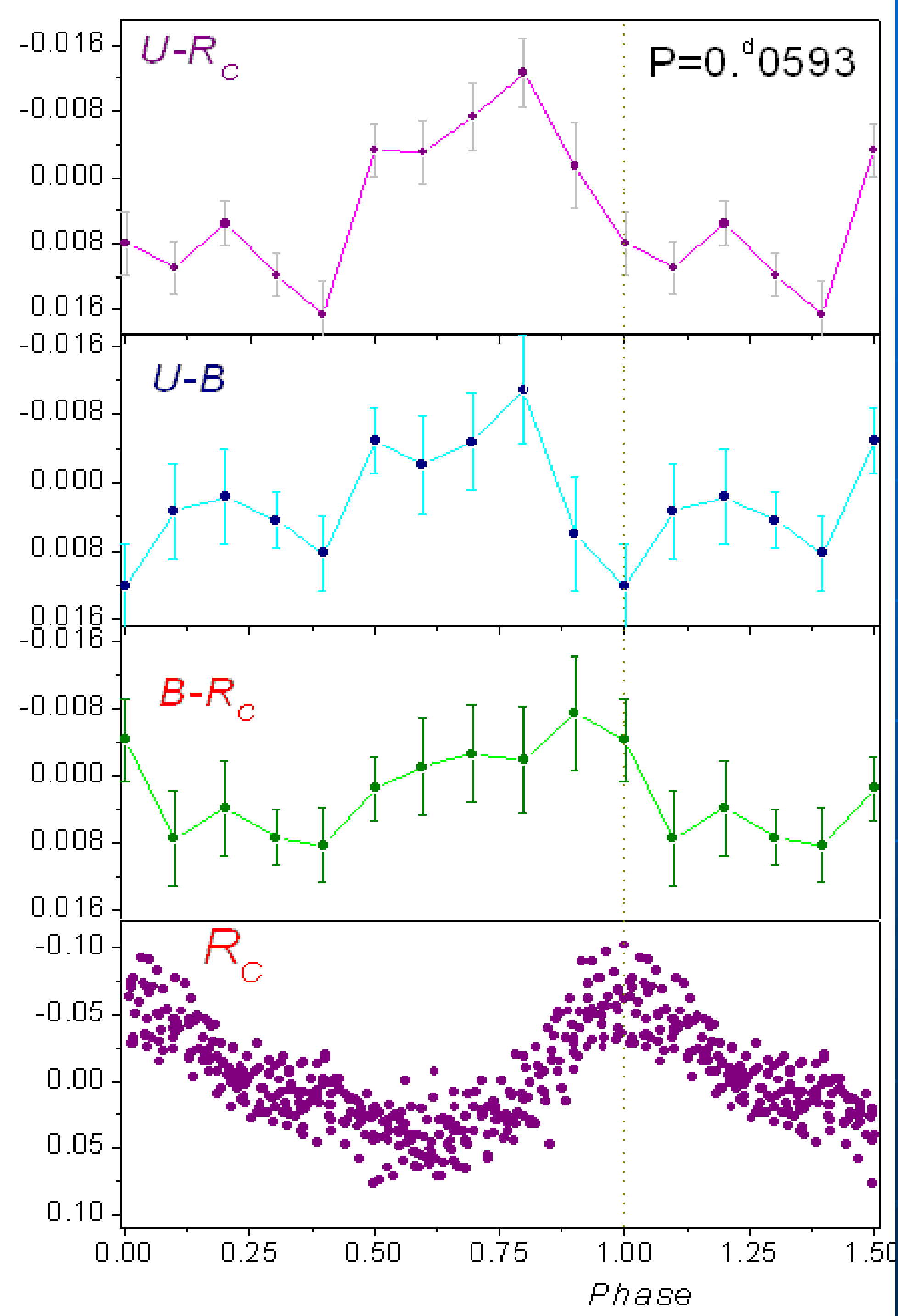

Some remarks

In the era of photoelectric observations the *UBV* photometry was developed. Now, at the time of CCD devices, most of observations of CVs are obtained in the *VRI*-passbands. Due to the lack of the ultraviolet *U*-passband data, we loose some information about the hot parts of the accretion disks, flowing matter and the white dwarfs. A significant fraction of the radiation comes from the disk and the white dwarf as well as from the accretion jet and disk collisions, which cause the hump before the eclipse in the majority of CVs. This hump has also the maximum amplitude in the UV region. We can conclude that observations in different passbands and primarily in the UV light, allow us to explain more confidently the physical processes taking place in the accretion disks.

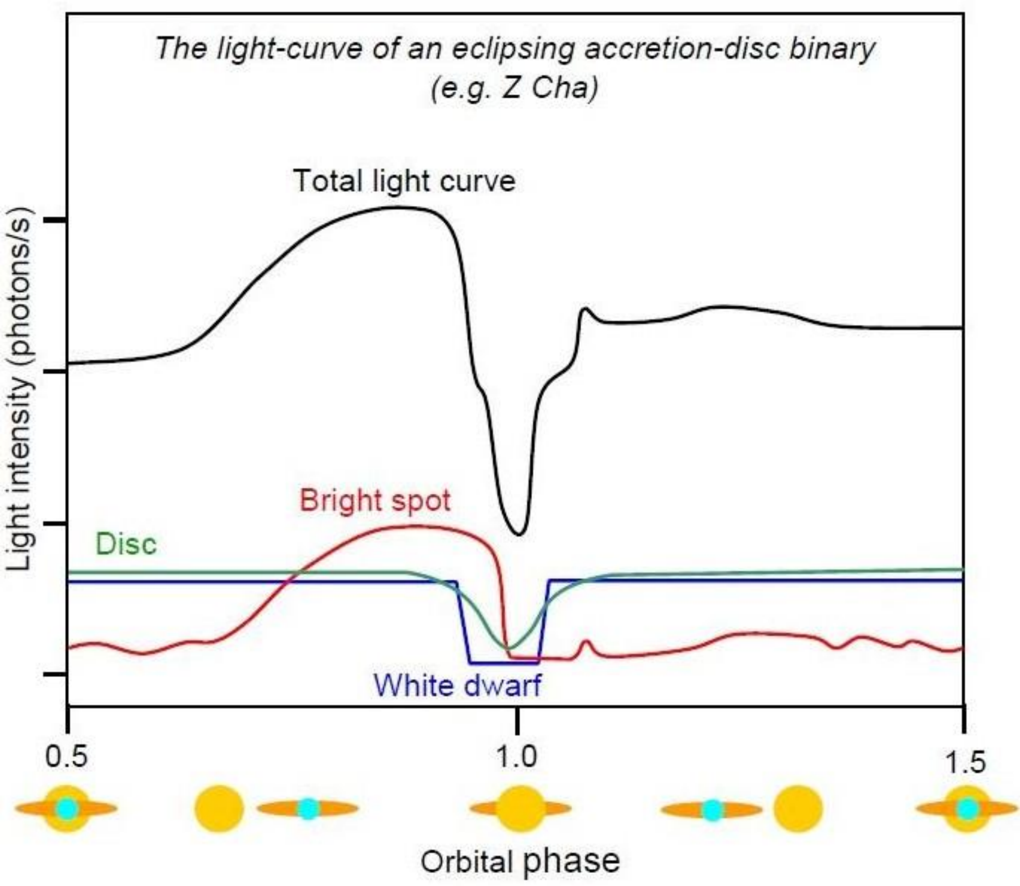

Bibliography

van Amerongen S., Bovenschen H., van Paradijs J., 1987: MNRAS 229, 245

Bailey J., 1980: MNRAS, 190, 119

Cannizzo J.K. & Kenyon S., 1987: Aph J., 320, 319

Echevarria J. & Jones D., 1983: Rev. Mexican Astron. Astrof., 5, 301

Golysheva P. & Shugarov S., 2014: Contrib. Astron. Observ. Skalnate Pleso, 43, 312

Kato T., Ishioka R., Isogai K., et al., 2016: PAS of Japan, 68, 107.

Kording E.G., Jester S., Fender R., 2008: - MNRAS, 383, 277

Maitra D., & Bailyn C.D., 2004: arXiv:astro-ph/0401212v1

Neustroev V.V., Marsh T.R., Zharikov S.V., et al., 2017: arXiv:astro-ph/1701.03134v2

Pavlenko E., Shugarov S., Baklanova D., Katysheva N., 2008: Bull. Crimean Astroph. Observ., 104, 109

Pavlenko E.P., Primak N.V., Shugarov S.Yu., 2002: Astrophysics, 45, 416